

# A compact design of a temperature gradient furnace for synchrotron microradiography

B Li<sup>1</sup>, H D Brody<sup>1</sup>, D R Black<sup>2</sup>, H E Burdette<sup>2</sup> and C Rau<sup>3</sup>

<sup>1</sup> Department of Metallurgy and Materials Engineering, University of Connecticut, Storrs, CT 06269-3136, USA

<sup>2</sup> National Institute of Standards and Technology, Gaithersburg, MD 20899, USA

<sup>3</sup> Frederick-Seitz Materials Research Laboratory, University of Illinois at Urbana Champaign, Argonne, IL 60439, USA

Received 27 October 2005, in final form 6 April 2006

Published 7 June 2006

Online at [stacks.iop.org/MST/17/1883](http://stacks.iop.org/MST/17/1883)

## Abstract

A compact, convenient and economic design of a temperature gradient furnace for synchrotron microradiography is described. The thermal control of the furnace, in terms of cooling rate and temperature gradient, was achieved by programmable temperature controllers, and provided necessary thermal conditions for real time observations of dendritic solidification in real alloys. The experiments at the Advanced Photon Source (APS), Argonne National Laboratory (ANL) demonstrate that the design is well suited to the melting and solidification of alloys with liquidus temperatures up to intermediate ranges ( $\approx 650$  °C), such as aluminium alloys. Real time observations with this furnace of dendritic solidification in Al–25 wt% Cu alloy by synchrotron microradiography show interesting and promising results.

**Keywords:** temperature gradient, furnace, synchrotron microradiography, solidification

(Some figures in this article are in colour only in the electronic version)

## 1. Introduction

In order to unambiguously understand alloy solidification processes, direct observations of growth of solid phases in the melt are preferred. The optical opacity of real alloys makes such observations extremely difficult. Therefore, observations usually have to be carried out on a sectioned metallographic sample after solidification is finished or interrupted by quenching, and one cannot record and observe the solidification process continuously. Such indirect observations have provided valuable insights towards the understanding of alloy solidification, but many mysteries still remain unsolved because there is no way to look through a solidifying alloy sample and observe the growth of dendrites in real time.

The high penetrating power of hard x-rays has made microradiography unique in observing internal structures of metallic materials [1–6]. Among the applications of

microradiography is the real time observation of alloy solidification [4–6]. Early observations were limited by the characteristics of the available x-ray sources, such as intensity and divergence and images were captured with limited resolution and contrast and only qualitative results were obtained [4–6]. More recently, the advancement in technology such as a digital camera coupled with solid-state imaging detectors that have fast response to x-ray photons and new types of x-ray sources, such as synchrotron radiation with extraordinarily high intensity, have stimulated renewed interest in real time studies of alloy solidification [7–15].

These experiments require an x-ray source, a solidification furnace and an x-ray optical system to record the images of the growing solid phase. The resolution of an optical system is determined by the quality of the x-ray source and the detector. Thus, it is very important to carefully choose an appropriate combination of the x-ray source and the detector, the discussion of which is beyond the scope of this paper. The

design and fabrication of a solidification furnace, on the other hand, plays a central part in the real time observations of alloy solidification.

In earlier experiments, dendrite coarsening and temperature gradient zone melting in Sn–13 wt% Bi alloy was studied using synchrotron radiation at the Cornell High Energy Synchrotron Source (CHESS) [12, 13]. For these experiments, a furnace was designed specifically to melt Sn–Bi alloys, which have liquidus temperatures below 250 °C [14]. In order to observe dendritic solidification in commercially important aluminium alloys, with liquidus temperatures around 640 °C, a new design was required.

In the present paper, we introduce a compact, economic design of a solidification furnace for synchrotron microradiography. The furnace can be used to melt alloys with moderately high liquidus temperatures such as aluminium alloys. It can also be used to solidify a sample with or without temperature gradient at a constant cooling rate. Moreover, an additional degree of freedom is available to perform 3D microtomography. We hope this design will be of interest to the synchrotron community.

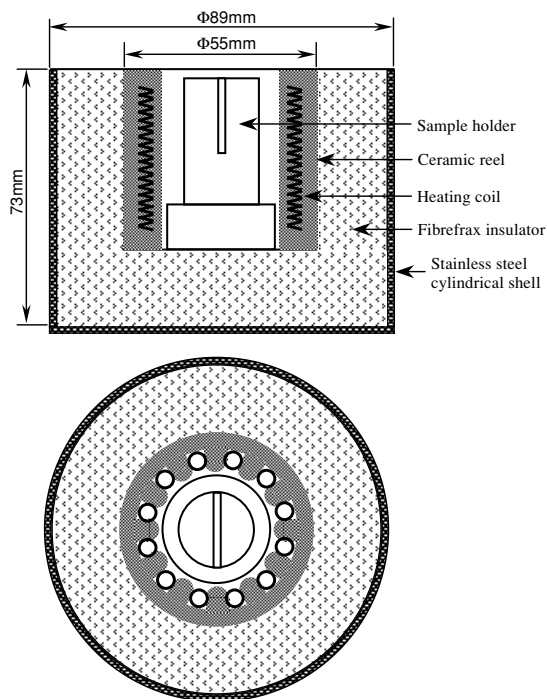
## 2. Design and fabrication

### 2.1. Furnace design

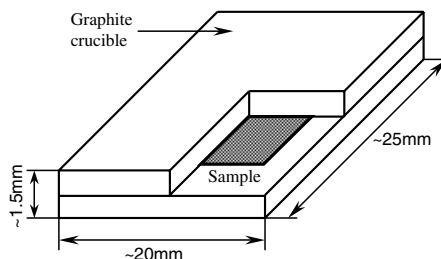
In addition to the desired flexibility in thermal control, such as controlled cooling rate and temperature gradient, a basic requirement is that the furnace cannot interfere with the x-rays during an experiment. The x-rays should impinge upon and pass through a solidifying sample and reach the detector without additional attenuation caused by the furnace. To satisfy this requirement, the furnace was designed with two identical, separate heaters, one on the top and the other at the bottom of the furnace with a clear central ring for the x-ray beam to enter and exit the sample.

Figure 1 shows schematically the bottom half of the furnace, which is composed of a stainless steel cylindrical shell, a ceramic reel, a heating coil (120 V, 60 W), a sample holder and a fibrefrax heat insulator. All items used in our fabrication were very inexpensive, typical laboratory supplies and scraps that can be found in many material laboratories. Major dimensions of the cylinder are also given in figure 1. The ceramic reel was wrapped with fibrefrax sheets and squeezed into the stainless steel cylinder. To slow down the oxidation of the heating coil at high temperatures, boron nitride (BN) adhesive was used to bury the coil inside the troughs of the ceramic reel. This also made the temperature distribution within the chamber more uniform. The fibrefrax is a good heat insulator and prevents heat loss and keeps the temperature of the stainless steel shell low. The sample holder was made from a piece of graphite. A slot was cut in the middle of the holder that fits the thickness of the sample assembly. Graphite has high heat conductivity but low oxidation resistance, so it is necessary to coat the surfaces of the sample holder with a thin layer of BN in order to slow down the oxidation of the graphite. This can be easily accomplished by applying commercial BN spray to the surfaces of the sample holder.

For radiographic imaging, no rotation of the sample was required, so the sample holder was designed and made to fit a thin slab sample–crucible assembly (figure 2). The crucible



**Figure 1.** Design of the bottom cylinder of the furnace. The furnace consists of two identical halves, one on the top and the other at the bottom, providing thermal control of the sample, which sits in the slot in the middle of the sample holder.



**Figure 2.** A schematic graph of the sample–crucible assembly. The sample was a thin slab of a Al–25 wt% Cu alloy sealed inside the graphite crucible. The surfaces of the graphite were coated with BN to slow down oxidation. The assembly resided in the slot of the sample holder inside the furnace during the experiment.

was made from graphite with all surfaces coated by BN, in order to slow down oxidation. Graphite was used because it has low absorption coefficient to the x-rays. Thus, major absorption was caused by the metal sample. A well-polished Al–25 wt% Cu sample was sandwiched between two graphite walls. In microradiography of solidification of Al alloys, protection of the melt from oxidation is usually not required. The convenience in sealing the sample in this way allows the assembly to be replaced by a fresh one after several thermal cycles when oxidation of the melt becomes a concern. The sample–crucible assembly resided in the slot of the sample holder inside the furnace during the experiment.

In future experiments, we expect to perform synchrotron tomography to observe growing dendrites in 3D in a rod-like sample. An extra degree of freedom of motion can be easily added to the current design and the sample assembly modified as needed as well.

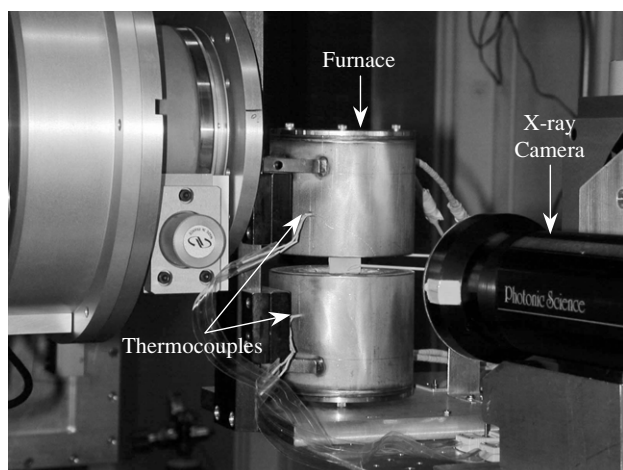


**Figure 3.** Experimental setup at the bending magnet line of sector 33-(UNICAT) of the Advanced Photon Source (APS) at Argonne National Laboratory (ANL).

During the experiment, the working position of the furnace was oriented vertically, as shown in figure 3. The sample was fixed between the top and the bottom heaters, and the x-rays passed through the sample through the space between the two cylinders. Thermocouples to measure the temperature of the sample could also be placed in the space between the two cylinders. The two cylinders were hinged to a dovetail sliding track, so that the distance between the two heaters was adjustable. This added extra flexibility for setting up the experiments and changing the samples between runs.

## 2.2. Temperature control

Crucial to the successful application of the furnace design was proper temperature control. In the studies of alloy solidification, in most cases we hope to observe steady-state dendrite growth. Thus, a constant temperature gradient and cooling rate are essential in these experiments. One way to achieve this is to translate the sample through the temperature gradient at a constant speed [7–9], and the temperature setup of the furnace remains unchanged during the experiment. This scheme allows observations to focus on the growth front of dendrites throughout the experiment, but introduces difficulties in the temperature measurement and disturbances to the solidifying sample. Another way is such that the sample remains still during solidification, but the sample is cooled at a constant cooling rate by bringing down the temperatures of the two heaters at the same pace [12–14]. This design is easier to implement and we employed this scheme for the thermal control of the furnace.

Because the two heaters were separated, the temperature inside each cylinder could be controlled separately and independently. If a temperature gradient was desired, a temperature difference could be set up for the two heaters. In the case that a uniform temperature was desired for the sample, we simply set the temperatures at the top and at the bottom to the same value. The obtainable temperature gradient of this design can be up to  $\sim 25.0\text{ }^{\circ}\text{C cm}^{-1}$ , and cooling rate up to  $\sim 8.0\text{ }^{\circ}\text{C min}^{-1}$ , without forced cooling.

As shown in figure 3, the temperatures of the furnace were measured by two type-K thermocouples (purchased as

unsheathed, 0.010 in or 0.25 mm in diameter for each wire). The thermocouples were sealed inside double-channelled ceramic insulators, and their beads were in contact with the sample holder and measured the temperatures at the top and at the bottom chambers of the furnace. The ceramic insulators were inserted into the chambers of cylinders through the stainless steel shell and the fibrefrax insulator. The measured temperatures were transmitted as process values to two temperature controllers. The controllers have an eight-segment temperature ramp/soak capability, and allow the temperatures of the two halves of the furnace to be ramped up or down linearly by controlling the power input to the heaters. The controllers are equipped with computer interface, and allow remote communication with each controller through an RS-232 communication port on a portable computer. The controllers are also featured with data logging with process values recorded at a maximum rate of one per second. During the experiment, the controllers and the furnace worked inside the x-ray station; remote control could be established by programming the controllers from a computer outside the station. Desired temperature cycles, such as constant temperature gradient and constant cooling rate, can be programmed and applied to the sample. Thus, steady-state growth can be obtained throughout the solidification range.

## 2.3. Tuning the furnace

The furnace was tuned in the laboratory to achieve good performance before it was installed at the synchrotron station to make real time observations of solidification of Al–25 wt% Cu alloy. The controllers are standard PID controllers (acronyms of Proportion, Integration and Derivative). The linearity of the cooling curves is greatly affected by the PID parameters. An inappropriate combination of the parameters gives rise to undesired oscillations in the cooling curve. Such a fluctuation in temperature causes changes to the dendritic structure and should be avoided. Following the standard procedure of tuning PID controllers, we can tune the controllers, find suitable parameters and change the settings of controllers to generate the desired thermal conditions, particularly the cooling rate. Figure 4 shows typical results for controlled cooling rates. The cooling rates are sufficiently linear to control the solidification process.

During the experiment, the temperature of the sample was also measured by the other two thermocouples attached to the top and the bottom of the sample. The temperatures were measured at two points 10.0 mm away on the sample along the temperature gradient. Figure 5 shows an example of the measured, actual cooling rate ( $4.0\text{ }^{\circ}\text{C min}^{-1}$ ) and temperature gradient ( $\sim 14.0\text{ }^{\circ}\text{C cm}^{-1}$ ) on the sample during the experiment. The linearity was sufficient. The fluctuation on the curves was caused by the loose contact between the thermocouple beads and the sample. As seen from figure 5, the top curve had better contact and was less noisy. In the case when accurate measurement matters, the noise can be eliminated by applying ceramic glue to the thermocouple beads, and rendering firm contact.

The temperature gradient can be easily reversed by changing the temperatures at the top and at the bottom. This allows the change of the growth direction of the dendrites.

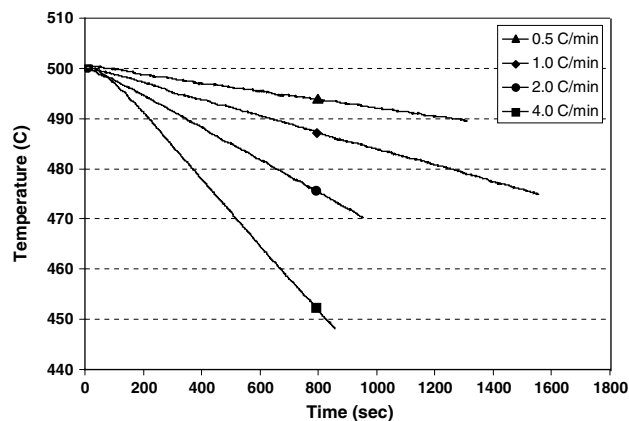


**Figure 4.** Linear cooling rates of the furnace obtained by programming the temperature controllers connected to the heaters residing at the top and at the bottom of the furnace.

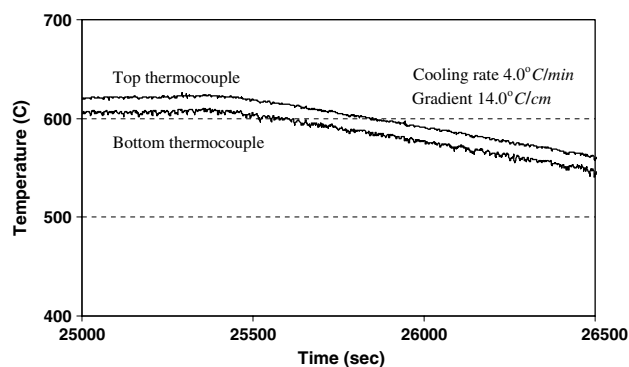
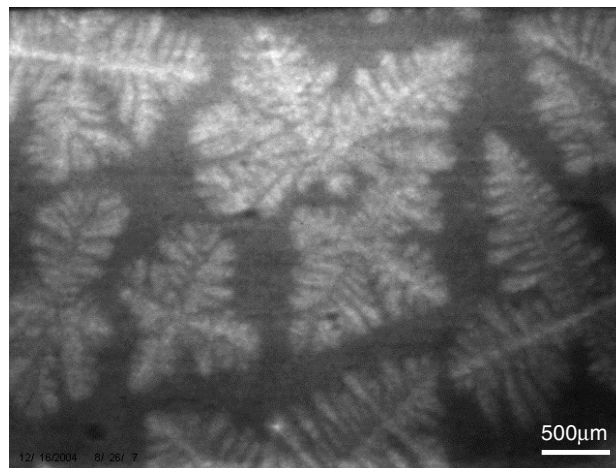


**Figure 5.** Measured, actual cooling rate and temperature gradient on the sample during the real time observation (cooling rate =  $4.0\text{ }^{\circ}\text{C min}^{-1}$ , gradient  $G = 14.0\text{ }^{\circ}\text{C cm}^{-1}$ ). The temperatures were measured by two thermocouples attached to the top and bottom of the sample, distanced  $10.0\text{ mm}$  along the gradient. The fluctuation was caused by the loose contact between the thermocouple beads and the sample.

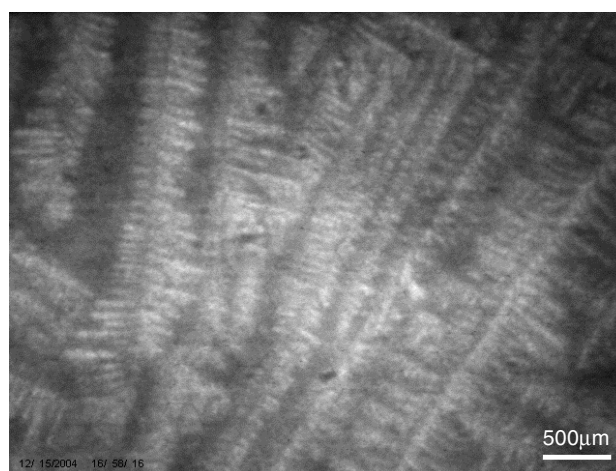
### 3. Real time observations by synchrotron microradiography

Real time observations of dendritic solidification of Al–25 wt% Cu alloy were performed at the third generation synchrotron source using state-of-the-art digital imaging systems at the bending magnet line of sector 33-(UNICAT) of the Advanced Photon Source (APS) at Argonne National Laboratory (ANL).

Figure 6 shows digital images of growing dendrites in Al–25 wt% Cu alloy. In figure 6(a), the cooling rate was  $2\text{ }^{\circ}\text{C min}^{-1}$  with a negligible temperature gradient. We can see that equiaxed grains nucleated and grew in the melt. Interestingly, as soon as these grains were formed, they quickly floated up to the top of the sample. This floatation indicates that the solid is less dense than the liquid, because the liquid was enriched with Cu. After the solidification started, the concentration of the first formed solid was much lower than the nominal concentration (25 wt% in Cu). The solute had to be rejected into the liquid, and the liquid was enriched with the solute. Not surprisingly, the density of the solid was



(a)



(b)

**Figure 6.** Digital images of growing dendrites in Al–25 wt% Cu captured by synchrotron microradiography. (a) Equiaxed grains. Cooling rate  $2.0\text{ }^{\circ}\text{C min}^{-1}$ , with negligible temperature gradient; (b) Columnar dendrites. Cooling rate  $2.0\text{ }^{\circ}\text{C min}^{-1}$ , temperature gradient  $\sim 20\text{ }^{\circ}\text{C cm}^{-1}$ .

less than that of the liquid. In figure 6(b), the cooling rate was  $2.0\text{ }^{\circ}\text{C min}^{-1}$  and the temperature gradient was about  $20.0\text{ }^{\circ}\text{C cm}^{-1}$ . The dendrites grew directionally, and a columnar dendritic structure can be seen.

A wide variety of experiments can be conducted with this flexible furnace design. Intriguing phenomena in alloy solidifications, such as dendrite coarsening, liquid flow and even 3D dendrite growth can be probed by performing real time microradiography.

### 4. Conclusions

We introduced a compact, inexpensive design and fabrication of a temperature gradient furnace for the real time observation of dendritic solidification in real alloys such as Al–25 wt% Cu by synchrotron microradiography. This design is capable of providing the necessary thermal conditions, e.g. linear cooling rates and temperature gradients, for alloy solidification including steady-state growth. The furnace will not interfere

with the x-rays and real time observations at the synchrotron facility show that the growing dendrites can be resolved and captured with promising results.

### Acknowledgments

The UNICAT facility at the Advanced Photon Source (APS) is supported by the US DOE under Award no. DEFG02-91ER45439, through the Frederick Seitz Materials Research Laboratory at the University of Illinois at Urbana Champaign, the Oak Ridge National Laboratory (US DOE contract DE-AC05-00OR22725 with UT-Battelle LLC), the National Institute of Standards and Technology (US Department of Commerce) and UOP LLC. The APS is supported by the US DOE, Basic Energy Sciences, Office of Science under contract no. W-31-109-ENG-38.

### References

- [1] Tzavaras A A and Flemings M C 1965 *AIME Trans.* **233** 355
- [2] Davis A M 1970 *Metallography* **3** 165
- [3] McLean M 1973 *Phil. Mag.* **27** 1253
- [4] Miller E W J and Beech J 1972 *In-situ* radiographic observations of alloy solidification *Metallography* **5** 298
- [5] Curreri P A and Kaukler W F 1996 *Metall. Trans. A* **27** 801
- [6] Sen S, Kaukler W F, Curreri P and Stefanescu D M 1997 *Metall. Trans. A* **28** 2129
- [7] Mathiesen R H, Arnberg L, Mo F, Weitkamp T and Snigirev A 1999 *Phys. Rev. Lett.* **83** 5062
- [8] Mathiesen R H, Arnberg L, Ramsoskar K, Weitkamp T, Rau C and Snigirev A 2002 *Metall. Trans. B* **33** 613
- [9] Mathiesen R H and Arnberg L 2005 *Acta Mater.* **53** 947
- [10] Thi H N, Jamgotchian H, Gastaldi J, Hartwig J, Schenk T, Billia B, Baruchel J and Dabo Y 2003 *J. Phys. D: Appl. Phys.* **36** A83
- [11] Yasuda H 2004 *J. Cryst. Growth* **262** 645
- [12] Li B, Brody H D and Kazimirov A 2004 *Phys. Rev. E* **70** 062602
- [13] Li B, Brody H D and Kazimirov A 2006 *Metall. Trans. A* **37** 1039
- [14] Li B 2004 *PhD Thesis* University of Connecticut
- [15] Rau C, Weitkamp T, Snigirev A, Schroer C G, Benner B, Kuhlmann M and Lengeler B 2002 Hard X-ray tomography with high resolution *Developments in X-ray Tomography III* ed U Bonse *Proc. SPIE* **4503** 14–22